



Biological control of biofilms on membranes by metazoans



Theresa Klein ^{a,1}, David Zihlmann ^{a,2}, Nicolas Derlon ^{a,b}, Carl Isaacson ^{a,3}, Ilona Szivak ^a, David G. Weissbrodt ^{a,b,4}, Wouter Pronk ^{a,*}

^a Eawag, Swiss Federal Institute of Aquatic Science and Technology, Department of Process Engineering, Dübendorf, Switzerland

^b Institute of Environmental Engineering, ETH Zürich, Zürich, Switzerland

ARTICLE INFO

Article history:

Received 24 April 2015

Received in revised form

28 September 2015

Accepted 30 September 2015

Available online 9 October 2015

Keywords:

Gravity driven membrane

Biofouling

Nematodes

Oligochaetes

Basal layer

Flux increase

Biological control

ABSTRACT

Traditionally, chemical and physical methods have been used to control biofouling on membranes by inactivating and removing the biofouling layer. Alternatively, the permeability can be increased using biological methods while accepting the presence of the biofouling layer. We have investigated two different types of metazoans for this purpose, the oligochaete *Aelosoma hemprichi* and the nematode *Plectus aquatilis*. The addition of these grazing metazoans in biofilm-controlled membrane systems resulted in a flux increase of 50% in presence of the oligochaetes (*Aelosoma hemprichi*), and a flux increase of 119–164% in presence of the nematodes (*Plectus aquatilis*) in comparison to the control system operated without metazoans. The change in flux resulted from (1) a change in the biofilm structure, from a homogeneous, cake-like biofilm to a more heterogeneous, porous structure and (2) a significant reduction in the thickness of the basal layer. Pyrosequencing data showed that due to the addition of the predators, also the community composition of the biofilm in terms of protists and bacteria was strongly affected. The results have implications for a range of membrane processes, including ultrafiltration for potable water production, membrane bioreactors and reverse osmosis.

© 2015 Elsevier Ltd. All rights reserved.

1. Introduction

Fouling in general and biofouling in particular are major limitations of membrane processes in water treatment. Many different measures are being exploited to control biofouling. For example, periodical flushing and disinfectants are used for cleaning of ultrafiltration membranes in the production of potable water (Nguyen et al., 2012). Membrane bioreactors (MBRs) usually feature aeration shear and periodical cleaning of the membranes (Nguyen et al., 2012; Zhang et al., 2007). Reverse osmosis (RO) units are equipped with extensive pretreatment processes and chemical cleaning is applied to limit biofouling in spiral wound modules

(Goosen et al., 2004). However, these chemical and physical measures for the reduction of biofouling have several disadvantages, such as the consumption of chemicals, the production of waste streams (Brepols et al., 2008), reduction of production time, and reduction of the membrane life time (Judd, 2008). Furthermore, these methods often fail to adequately control biofouling, for example while organisms can develop a resistance against cleaning agents (Calderon et al., 2011; Mahendran et al., 2011).

Alternatively, biology-based strategies can be considered for the control of biofouling (Malaeb et al., 2013), for example using quorum quenching, enzymatic disruption, energy uncoupling, cell wall hydrolysis and the use of microbial predation and bacteriophages. In this study we focus on the use of specific predators (oligochaetes and nematodes) under controlled conditions, with the goal of modifying the structure of fouling layers and reducing its hydraulic resistance. Predators are metazoans, which belong to the kingdom of Animalia. Metazoans are heterotrophic, eukaryotic organisms and in contrast to bacteria, they are multicellular. Oligochaeta is a subclass in the phylum of Annelida, which includes many types of aquatic and terrestrial worms. Nematoda is a separate phylum within the kingdom of Animalia, which inhabit a broad range of environments. Nematodes are ubiquitous and they have an important effect on global ecosystems. In deep sea, nematodes

* Corresponding author.

E-mail address: wouter.pronk@eawag.ch (W. Pronk).

¹ Present address: Institute for Corrosion Protection (IKS) Dresden Ltd, Dresden, Germany.

² Present address: Department of Civil, Environmental and Geomatic Engineering, ETH Zürich, Zürich, Switzerland.

³ Present address: Environmental, Earth and Space Studies, Bemidji State University, Bemidji, MN, USA.

⁴ Present address: Department of Biotechnology, Delft University of Technology, Delft, The Netherlands and Center for Microbial Communities, Department of Chemistry and Bioscience, Aalborg University, Denmark.

account for 90% of the abundance of multicellular organisms impacting marine soft bottoms by mucus secretions (Riemann and Helmke, 2002; Danovaro et al., 2008). A great number of marine nematodes were reported to agglutinate detrital particles, thus forming lumps or burrows in the size of a few millimeters (Riemann and Helmke, 2002). While many metazoan species are natural consumers of biomass in the benthic layers of ecosystems, the activity of different types of higher organisms were reported to result in a reduction of the mass of biological sludge (Tamis et al., 2011; Wu et al., 2008). Specifically, the effect of oligochaetes has been demonstrated in several activated sludge systems. For instance, in fluidized bed biofilm reactors, a decreased biomass yield and an increased oxygen consumptions have been linked to predation by oligochaetes (Li et al., 2013). Additionally, olichogaetes such as *Aulophorus furcatus* and *Aelosoma hemprichi* were applied for the reduction of secondary sludge in so-called “worm reactors”, which are biofilm reactors based entirely on oligochaetes (Elissen et al., 2008; Tamis et al., 2011; Wei et al., 2009). Furthermore, the occurrence of nematodes has been related to the porous, sponge-like structures of the fouling layer and flux stabilization in membrane bioreactors (MBRs) (Jaborinig and Podmirseg, 2015). On the other hand, the presence of *Aelosoma hemprichi* in MBRs has been shown to lead to a decrease in phosphorus removal, an increase of soluble microbial products (SMP) and a higher membrane fouling rate (Menniti and Morgenroth, 2010; Wang et al., 2011). In activated sludge reactors, the occurrence of oligochaetes can be problematic since they reduce the sludge amount and activity (Song and Chen, 2009). Also, nematodes have been reported to influence biological reactors. Grazing by nematodes has been shown to reduce biomass growth by 45% in a biotrickling filter (Seigneur et al., 2004), while the abundance of different nematode species in a wastewater biofilter reactor was found to be dependent on the operating conditions (Bergtold et al., 2007).

While the influence of specific metazoans on the sludge reduction in MBRs and activated sludge systems has been investigated reasonably well, a limited amount of studies is available on their influence on membrane filtration processes. It has been shown that metazoans can increase flux and modify biofilm structure in biofilm-controlled membrane filtration (Derlon et al., 2013), but only indigenous metazoans were studied. Böhme et al. (2009) showed that specific types of metazoans (*Dexiostoma*, *Vannella*, *Chilodonella*) impact the morphology of biofilms grown on fixed surface. However the impact on membrane biofilms and their permeability was not investigated. Based on the literature presented above, it is possible that intrusion of metazoans in membrane biofilms could have both positive and negative effects on flux, depending on the type of organisms which are entering the system with the feed water. In the present study, we intended to engineer the biofilm by spiking specific types of nematodes and oligochaetes. The role of these organisms on the permeability, morphology and ecology of the biofilms was investigated by spiking them into biofilm systems free of metazoans. To this end, a dead-end operated, gravity driven membrane system was used (Peter-Varbanets et al., 2012; 2010). In order to provide reproducible conditions, a bacterial biofilm free of metazoans was built up filtrating autoclaved river water until the flux stabilized. After flux stabilization, two different isolated species of metazoans were added to the feed water, namely oligochaetes, sp. *Aelosoma hemprichi* and nematodes, sp. *Plectus aquatilis* (see Fig. 1). The impact on flux was monitored and the morphology of the biofilm was observed using different optical techniques. After completion of the experiment, the community composition of the biofilms was analyzed using amplicon pyrosequencing.

2. Materials and methods

2.1. Experimental set-up

The membranes were hydrophilized polysulfone ultrafiltration membranes with a nominal molecular weight cut-off (MWCO) of 100 kD, provided by Microdyn Nadir, Wiesbaden, Germany (type US100). In order to remove conservation agents, membranes were rinsed overnight in Nanopure water and the permeability was tested with Nanopure water before start of the operation. A specific design of flow cells was used in which the flat membranes are clamped using screws and O-rings. These modules are suitable for in-situ observation of the fouling layer, as shown in Fig. S1 (Supplementary material).

The effective membrane area of each flow cell was 0.00231 m², the height of flow channel (membrane surface to cover glass) amounts to 1.5 mm. The systems were operated in a controlled temperature environment (21–22 °C). The flow cells were operated in dead-end mode, except during the flushing event to remove the biofilm (see below). As recommended by the manufacturer, membrane flow cells were rinsed with nanopure water in a permeation mode during 24 h, after which the clean water flux was determined.

Water fluxes were measured gravimetrically with balances connected to a supervisory control and data acquisition (SCADA) system, whereby the weight was converted to volume. Fluxes were calculated on-line with time intervals of 1 h in the first 46 h of operation, and 4 h afterwards.

Ten membranes flow cells were operated in parallel with a constant hydrostatic pressure of 61.5 mbar. The modules were positioned in the dark at an angle of 45° to the surface of the shelves. The set-up was cleaned with a hypochlorite solution (50 ppm) before inserting the membranes. The clean water permeability was determined with nanopure water. The average clean water permeability of the membranes was 663 L/(m²h). Autoclaved water (ACBW) from the Chriesbach river (Dübendorf, Switzerland; WGS84 coordinates 8.61131, 47.40466) was used as feed water for biofilm growth on membrane modules during the whole experiment. The TOC value and composition of Chriesbach water were reported before: the typical TOC range is 2–3 mg/L (Peter-Varbanets et al., 2012), with NOM fractions as shown by Peter-Varbanets et al. (2010). A volume of 5 L of river water was autoclaved before use at 121 °C core temperature during at least 1 h in order to inactivate all higher organisms. The feed tanks were deliberately kept open to the air, in order to allow bacterial intrusion, growth and formation of biofilms. After 24 days of biofilm growth the modules were disconnected from the setup, flushed and filled with a NaCl salt solution (5 g/L) which was removed the next morning by flushing with autoclaved river water, in order to remove higher organisms that had intruded the system, probably by spores in the air (type of higher organisms could not be identified). During day 30–32, again a NaCl salt solution (5 g/L) was added to the control systems in order to eliminate higher organisms, since intrusion of a small amount of higher organisms was observed in these systems.

Hydraulic resistances of membrane and fouling layer were calculated using the resistance in series model and Darcy's law after normalization to 20 °C using the correlations as shown below (Crittenden et al., 2012).

$$k_{tot} = k_m + k_f \quad (1)$$

$$J = \frac{\Delta P}{\mu \cdot k} \quad (2)$$

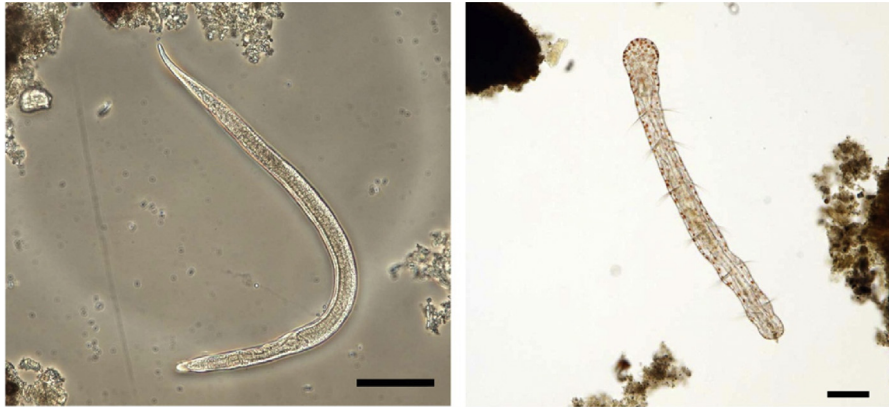


Fig. 1. Microscope images of the higher organisms used for inoculation: in the left panel the nematode *Plectus aquatilis* and in the right panel the oligochaete *Aelosoma hemprichi*. The scale bar represents 100 μm .

$$J_{T_1} = J_{T_2} (1.03)^{T_1 - T_2} \quad (3)$$

where k_m , k_f and k_{tot} are the hydraulic resistances of membrane, fouling layer, and total resistance (m^{-1}), J is the flux ($\text{m}^3 \text{m}^{-2} \text{s}^{-1}$), ΔP is the transmembrane pressure ($\text{kg s}^{-2} \text{m}^{-1}$), μ is the dynamic viscosity ($\text{kg m}^{-1} \text{s}^{-1}$) and T is the temperature (K).

2.2. Isolation and inoculation of higher organisms

The organisms that were used for this experiment naturally occur in the Chriesbach river. The nematodes, *Plectus aquatilis*, were isolated from the Chriesbach river according to a procedure derived from Isaacson (2015), as described below. Nematodes were grown in batch cultures in aerated water from the Chriesbach river amended with protozoan pellets and wheat seeds (both from Carolina Biological Supply, Burlington, NC), hemoglobin (Calbiochem, Darmstadt, Germany) and cholesterol (Alfa Aesar, Karlsruhe, Germany). To separate the nematodes from the culture media, the culture was first concentrated by centrifugation for 5 min at 500 g. The concentrate was then repeatedly resuspended in 60% sucrose and centrifuged for 20 min at 500 g, and the nematodes were collected at the top of the sucrose layers (Böhme et al., 2009; Isaacson et al.). After separation on sucrose gradients, nematodes were resuspended in Chriesbach river water. The nematodes were identified by DNA barcoding at the University of Bielefeld (Germany). The LSU and SSU were determined to be that of the bacteria feeding nematode specie *Plectus aquatilis*. Under the microscope, these nematodes are transparent, and are between 200 μm and 1 mm in length, and have a diameter of about 20 μm (Fig. 1). They move by curling and stretching.

Oligochaetes affiliating with *Aelosoma hemprichi* were isolated by microscopic pipetting from biofilms grown with untreated Chriesbach river water. These annelids are characterized by red oily drops and setae (hairs) over the whole body (Fig. 1). The length of these organisms is between 500 μm and 1 mm long and the diameter about 50 μm . The oligochaetes were isolated from biofilm grown with untreated Chriesbach river water by careful pipetting under the microscope the day before inoculation. To our knowledge, this procedure is the best possible practice developed for isolating oligochaetes. It allows for a very significant enrichment of oligochaetes, but cannot provide a complete purification of these organisms. The day of inoculation the organisms were divided into three drops of about 30 organisms per drop of SA-CBW water. These drops were added carefully on the biofilms grown with ACBW water.

The effect of nematodes was investigated in low and high amounts of approximately 100 and 900 organisms in two sets of modules called NL1/NL2 and NH1/NH2, respectively. Amounts of 20–30 oligochaetes were inoculated in three membrane modules hereafter referred to as O1, O2 and O3. After inoculation the membrane modules were reconnected to the system and fed with ACBW water. The two control modules C1 and C2 were operated with ACBW without inoculation of higher organisms. In addition, a third control module (CC) was operated with ACBW mixed with cycloheximide in a concentration of 100 mg/L, in order to inhibit the growth of higher organisms. Because the top glass of the latter system was broken on day 40, the data of this control could only be used until this date. During the period after inoculation, the biofilm structures were monitored two times per week using stereo microscopy and OCT (optical coherence tomography) after disconnecting the flow cells from the system without disassembling them.

2.3. Hydraulic biofilm removal by forward flushing

On day 50, the membrane systems C2, NL1, NH1 and O1 were disconnected and the biofilm was removed for pyrosequencing. The detached biofilm fractions were stored in 2 mL Eppendorf tubes at -80°C pending molecular analyses. C1, CC, NL2, NH2, O2 and O3 were continued. In order to investigate the structure of the basal layer, the latter modules were flushed on day 62 using a cross-flow pump without permeation, at a flow rate of 1.47 L/min, corresponding to a linear flow rate of 0.817 m/s, a shear rate of 2.50 Pa and a Reynolds number of 1024.

2.4. Optical coherence tomography (OCT) and stereo microscopy

The structure of biofouling layer was examined at meso-scale with OCT and at macro-scale with stereo microscopy.

An Optical Coherence Tomograph (OCT) (model 930 nm Spectral Domain, Thorlabs GmbH, Dachau, Germany) with a light-source wavelength of 930 nm was used to investigate the mesoscale structure of the biofilm by direct imaging through the cover glass of the flow cells. For the determination of biofilm roughness, 20 randomly positioned images were taken per module and analyzed with a Matlab[®] image analysis routine, as described previously (Derlon et al., 2012) and the roughness was averaged among all modules of a specific metazoan community. Biofilm formation was monitored on a macro-scale by stereomicroscope (OLYMPUS SZX10 with DP72 digital microscope camera and software, Schweiz.) using

tile-imaging mode with 0.63× objective.

2.5. Confocal laser scanning microscopy (CLSM)

After flushing the biofilm on day 62 as described above, the remaining biofilm (“basal layer”) was fixated with 3.7% (v/v) stabilized formaldehyde (PFA) (Sigma Aldrich, Germany) solution in ACBW and incubated on ice for 1.5 h. After the fixation step, GDM filters were stored in ACBW at 4 °C for not more than 2 weeks. The fixated membranes were cut carefully in pieces of 1 × 1 cm and stained during 15 min with Sypro Orange (S-6650, Invitrogene, Life Science Technology, USA) for protein staining, or Sytox Green (S-7020, Invitrogene, Life Science Technology, USA) for DNA staining (dilution factor of the original stain solution 1:1000). Five randomly chosen image-series of fields of view (FOV's) in XYZ dimensions were acquired by confocal laser scanning microscopy (CLSM, Leica, SP5, Wetzlar, Germany). 488 and 543 nm laser lines were used to detect Sypro Orange or Sytox Green respectively. A 25× water dipping objective (NA 0.95) and LAS AF 2.7v. (Leica, Wetzlar, Germany) imaging software were used for image acquisition. For one channel the same setting of the detector (PMT) sensitivity was kept for every field of view (FOV). The most representative images are shown. Z-stacks recorded with the CLSM were processed using ImageJ (<http://imagej.nih.gov/ij/>) to quantify the change in the biofilm density (%) over the biofilm depth. The image processing was as follows: (i) conversion of the CLSM images into 8-bit images; (ii) binarization of the 8-bit images by automatic thresholding using the triangle algorithm; (iii) quantification of the biofilm density for each Z-position. For each biological condition, multiple randomly chosen images were taken and analyzed, and the average value of biofilm density was calculated as a function of Z for each system. For the control system (C1) 6 different randomly chosen images were analyzed, for the system with a high dose of nematodes (NH2) 5 different images were analyzed, for the system with a low dose of nematodes (NL2) 5 different images were analyzed, and for the systems with oligochaetes (O2 and O3) in total 6 images were analyzed.

2.6. Amplicon pyrosequencing and numerical analyses of eukaryal and bacterial community compositions of biofilm layers

Bacterial tag-encoded FLX amplicon pyrosequencing (bTEFAP) analyses (Sun et al., 2011) were conducted in order to characterize the eukaryal and bacterial diversities, underlying the biofilm layers from each GDM module at the end of the experimental phase (>50 days). The main objectives of these analyses were (i) to determine whether the controls were free of nematodes and oligochaetes and (ii) to assess whether the biological treatments with nematodes and oligochaetes were related to specific impacts on the microbial compositions of the biofilms in addition to effect on the physical structures and water fluxes.

Genomic DNA (gDNA) was extracted and purified from the detached biofilms fractions using the FastDNA SPIN Kit for Soils (MP Biomedicals, USA) with adaptation of the manufacturer's protocol with 4 series of 40 s of bead-beating at 6 s⁻¹ and intermediate idle periods of 5 min on ice. The concentration and quality of the gDNA extracts were assessed with a NanoDrop UV-VIS spectrophotometer (ThermoScientific, USA). The gDNA extracts were diluted to 20 ng μL⁻¹ prior to submission to Research and Testing Laboratory (Lubbock, Texas) for bTEFAP analysis targeting 3000 reads on average.

The universal primer pairs Bact341F (5'-CCTACGGGNGGCWGCAG-3')/Bact785R (5'-GACTACHVGGGTATCTAATCC-3') and Euk555F (5'-AGTCTGGTCCAGCAGCCGC-3')/Euk1055R (5'-CGGCCATGCACCACC-3') were used for targeted amplification by

polymerase chain reaction (PCR) of fragments of 400–500 bp of the v3–v4 and v4 hypervariable regions of the bacterial 16S and eukaryal 18S rRNA gene pools, respectively. The coverage and specificity of these primer pairs were tested *in silico* against the SILVA rRNA gene database of reference sequences (Camacho et al., 2009; Quast et al., 2013) prior to bTEFAP analysis. The denoised sequencing datasets were mapped against NCBI BLASTn+ (Johnson et al., 2008) for phylogenetic affiliations to closest bacterial and eukaryal relatives. The community profiles were presented as relative abundances of populations within the kingdoms of Bacteria, Animalia and Protista (or Eukaryota).

Hierarchical clustering and unconstrained ordination numerical analyses were computed in R (R Foundation for Statistical Computing, Vienna, Austria) using the vegan package according to Borcard et al. (2011) and Weissbrodt et al. (2014) in order to identify distances in overall community patterns obtained for the different biofilm systems subjected to treatments with nematodes and oligochaetes. Hierarchical clustering was performed using the Ward's minimum variance method. Principal component analysis (PCA) was computed in order to represent the major features of the datasets in the reduced ordination space delineated by the first two PC1 and PC2 axes that explained between 52 and 82% of the variance between the samples of the bacterial and eukaryal sequencing datasets, respectively. In both approaches, Hellinger distances between community datasets were considered in order to cope with species abundance data.

The molecular and numerical analyses were conducted with biological duplicates (two untreated control systems and two flow cells treated with nematodes) and triplicates (three flow cells treated with oligochaetes), as well as technical triplicates on the bTEFAP method with DNA extracts for each set of treatment, namely C2, NL1, NH1 and O1.

3. Results and discussion

3.1. Influence of metazoans on permeability and flux

Ten parallel membrane systems were fed with autoclaved Chriesbach water (ACBW) in a dead-end mode. In the initial period of operation, the flux in all systems decreased rapidly and stabilized to a value of around 3.6–6.9 L/(m²h) (Fig. 2), which corresponds to stable flux values previously reported for river water (Peter-Varbanets et al., 2010). During day 13–14, the pump feeding ACBW to the head water tank broke down, which resulted in a reduction of the water head and consequently a temporary flux reduction. After inoculation (on day 24), the flux of all systems including controls increased during the first few days, presumably due to relaxation of the biofilm (relaxation was described by Peter-Varbanets et al. (2012)). Afterwards, the flux in the systems dosed with oligochaetes increased to reach a value of 9.2–12.5 L/(m²h) (as indicated by the shaded box). For the systems inoculated with nematodes, the flux increase was dependent on the dosed amount of nematodes. In the case of the low dose (100 organisms per flow cell), the flux increase started later and the stable flux level was slightly lower (14.0–17.7 L/(m²h)) as compared to the high dose (17.5–20.8 L/(m²h)). In the control systems, the flux displayed some initial variability and reached a value of 5.7–8.8 L/(m²h) in the final period of operation as indicated by the shaded box. Thus, in comparison to the control operated with a bacterial biofilm, the flux in the systems with oligochaetes was increased by 50% (from 7.25 to 10.85 L/(m²h) on average). In the case of a low dose of nematodes the flux was increased by 119% (from 7.25 to 15.85 L/(m²h)) while the flux increased by 164% in case of a high dose of nematodes (from 7.25 to 19.15 L/(m²h) in average).

The results show a clear impact of the presence and type of

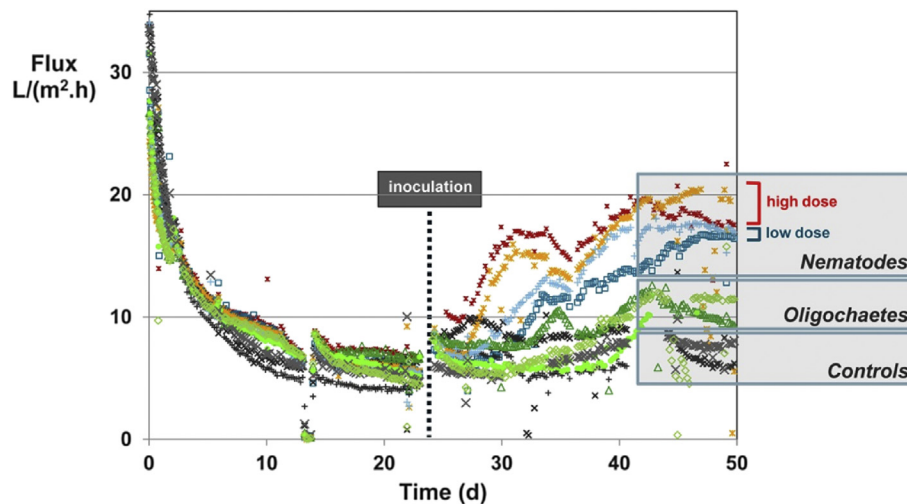


Fig. 2. Flux in different membrane flow cells operated in parallel. All systems were fed with autoclaved river water until day 24, when inoculation was carried out with different types of metazoans except for the control systems. Outliers were caused by mechanical problems. The flux decrease at day 13–14 was caused by breakdown of the feed water pump.

metazoans on the permeability of the biofilm. In case of the high dose of nematodes, the total hydraulic resistance calculated on basis of the stable flux amounts to $1.11\text{--}1.32 \times 10^{12} \text{ m}^{-1}$ (see Table S1 and Fig. S2). While the pure water flux (flux with nanopure water) determined before the start of the experiment was $40.75 \text{ L}/(\text{m}^2\text{h})$ on average, the membrane resistance can be calculated as $5.68 \times 10^{11} \text{ m}^{-1}$ and thus, the resistance of the fouling layer is $5.45\text{--}7.55 \times 10^{11} \text{ m}^{-1}$. In comparison, the resistance of the fouling layer in the control systems amounts to $2.06\text{--}3.49 \times 10^{12} \text{ m}^{-1}$. Thus, due to the influence of metazoans, the resistance of the fouling layer is reduced by up to 84% and reaches a value comparable to the membrane resistance. In case the presence of metazoans and the high flux can be maintained during longer periods of time, this principle can be used to increase the productivity of decentralized membrane systems, although these systems are feasible also at low flux values (Peter-Varbanets et al., 2011). In addition, it might also provide an interesting perspective for large scale, centralized systems. The resistance is at least as low as in conventional membrane processes (Crittenden et al., 2012), although no flushing or cleaning is applied in our case. While the transmembrane pressure is higher in conventional processes, the flux is correspondingly higher (around $50\text{--}100 \text{ L}/(\text{m}^2\text{h})$) compared to up to $20 \text{ L}/(\text{m}^2\text{h})$ in the presence of nematodes, which results in a lower required membrane surface area. However, this difference may largely be compensated by the absence of cleaning and flushing, which will reduce both the investment and variable costs of the process as well as the lower pressure head, which reduces the energy consumption. Therefore, gravity driven membranes are expected to be economically competitive against conventional processes even for large-scale applications whilst providing environmental benefits in terms of lower energy and chemicals consumption. Furthermore, the pronounced influence of metazoans may be utilized to reduce the resistance in MBRs (see Section 3.4).

3.2. Influence of metazoans on structure of the fouling layer and basal layer

In addition to the impact on flux, the dosing of metazoans also led to specific changes in the morphology of the bio-fouling layer, which in this context is also referred to as biofilm. Stereo microscopy and optical coherence tomography (OCT) enabled in-situ characterization and monitoring of the 3-dimensional structure of

the biofilm on different scales. OCT cross-sections (Fig. 3) show that in the control systems the structure of the biofilm remained relatively homogeneous and no substantial detachment of biofilm occurred. In the systems amended with nematodes, biofilm release from the membrane surface is visible six days after inoculation (day 30), while in a later stage (day 49) a highly heterogeneous biofilm remains with relatively large, patchy biofilm structures. It can also be observed that on day 49, a large proportion of the membrane area was not covered by biofilm. The system with oligochaetes exhibited a heterogeneous biofilm structure, but the uncovered area of membrane was less pronounced than in the nematode system.

On basis of the 2-dimensional OCT images the roughness and thickness of the biofilm was determined using image analysis software at many different locations chosen randomly during the final period of operation (40–50 days). As shown in Fig. 4, both the biofilm thickness and the biofilm roughness of the systems inoculated with metazoans is significantly higher than in the controls, with a thickness ranging between 112 and $171 \mu\text{m}$ as compared to $65 \mu\text{m}$ in the controls, and a roughness of $61\text{--}105 \mu\text{m}$ as compared to $16 \mu\text{m}$ in the controls while no significant difference could be observed between the systems spiked with different types or different doses of metazoans. These results are in accordance with previous investigations, where the presence of metazoans was found to result in a more heterogeneous morphology of membrane biofilms (Derlon et al., 2013, 2012).

The structural changes observed by OCT also occur on a macro scale as analyzed by microscopy. A heterogeneous structure and local release of biofilm is observed in nematode systems (Fig. S3, b–c), while the biofilm fully covers the membrane area in the control (Fig. S3, a). Oligochaetes habitats are observed as accumulations of debris around 1.5 mm in size (Fig. S3, d–e), which is in accordance with agglutination by metazoans as described by Riemann and Helmke (2002).

In order to characterize the basal layer, the loosely attached part of the biofilm was removed from the membranes by applying a cross flow at a relatively high shear rate of 2.50 Pa at the end of the experiment. The remaining strongly attached, shear resistant layer of biofilm is defined as the “basal layer” (Böhme et al., 2009; Pechaud et al., 2012). The basal layer structure was examined by confocal laser scanning microscopy (CLSM) after protein staining with Sypro Orange (Fig. 5) and DNA staining with Sytox Green

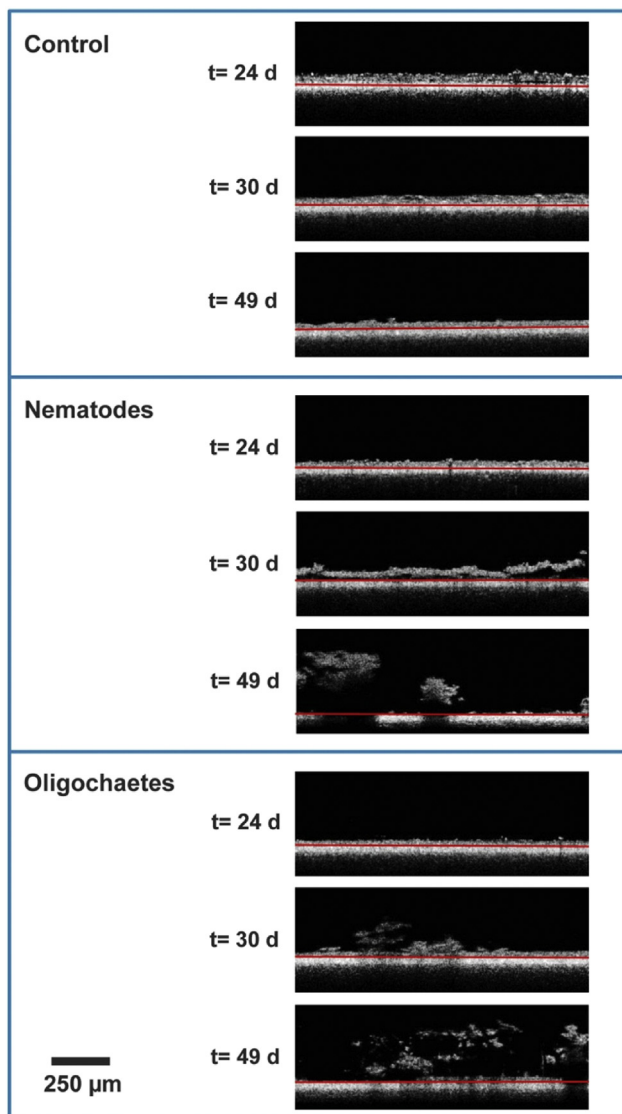


Fig. 3. Representative lateral views (cross sections) of biofilms recorded with OCT for the control system and the flow cells inoculated with nematodes (high dose) and with oligochaetes. The red lines delineate the interface between the membranes (below) and the biofilm (above the line). The scale bar represents 250 μm .

(Fig. S4). According to the top views and the cross sections presented (Fig. 5), the density of the basal layer in the control systems (a, e) is significantly greater than in the nematode systems (b–c, f–g). Also for the DNA staining (Fig. S4) the basal layer of the control appears to be thicker and denser than in presence of metazoans, while the difference between oligochaetes and nematodes seems to be less evident. A possible explanation for the difference between protein and DNA staining is that there is a difference in feeding and excretion pattern between the different metazoans, leading to similar amounts of cells but less proteins in the case of nematodes. The density of the basal layer of the oligochaetes system is somewhat lower than the control, but higher than the nematodes system. Based on 20 randomly chosen CLSM images of each membrane system, basal layer density profiles were calculated, as shown in Fig. 6. This figure shows that the highest density near the membrane occurs for the control system, with a basal layer thickness of around 20–25 μm . In the oligochaetes system, the general biofilm

intensity is lower than in the control, while the total thickness is somewhat higher (20–30 μm). The clearest effect on basal layer is observed in the systems inoculated with nematodes. The intensity and thickness of the basal layer was significantly reduced in comparison to the control system. Comparing the high and low dose of nematodes, the high dose resulted in a lower density than the low dose of nematodes. Similarly, Böhme et al. (2009) showed that protists influence the basal layer properties and morphology of biofilms grown on non-permeable surfaces, with varying basal layer thicknesses for different protist communities.

3.3. Influence of metazoans on biofilm community

Amplicon pyrosequencing analyses of the biofilms were first used to show that higher organisms of the kingdom of Animalia were not detected in all control systems (Fig. S5-A). The combination of molecular analyses targeting the 18S and 16S rRNA gene pools with numerical methods further revealed that the presence of higher organisms such as nematodes and oligochaetes in the GDM modules did not only impact the permeate flux and biofilm architectures, but also resulted in significant differences in the underlying eukaryal and bacterial community structures. The exploration of the sequencing datasets with hierarchical clustering and principal component analysis (PCA) highlighted significant effects of nematodes and oligochaetes on the community compositions within the kingdoms of Protista and Bacteria (Fig. 7). For every kingdom, the community compositions of the biofilms treated with higher organisms was significantly distant from the untreated controls. For both the kingdoms of Animalia and Bacteria, the community compositions were specifically clustered according to the type of biological treatment.

3.4. Mechanistic model and perspectives for application

In summary, our results show that the presence of metazoans influences (I) the permeability of the fouling layer, (II) morphological aspects of the biofilm and the basal layer and (III) the community composition of the biofilm. The biofilm structure (thickness and roughness) in presence of metazoans is significantly different from that in the control systems, whereby no significant structural differences between nematodes or oligochaetes could be shown (Fig. 4). However, significant differences could be observed between the basal layer of nematodes and oligochaetes systems (Figs. 5 and 6).

Metazoans influence the composition of bacteria and protists as a result of their feeding patterns. Members of the genus *Aelosoma* are reported to feed on fine organic particles (Dodds, 2002), while *Plectus aquatilis* is a predator which grazes on bacteria (Gaudes et al., 2013). Furthermore, it has been shown that excretion products from nematodes influence the microbial community in sediments (Gaudes et al., 2013). Predation can directly influence the bacterial community, while excretion and detritus feeding influence the substrate composition, which in turn also impacts the community of bacteria and protists. The feeding pattern also can influence the structure of the biofilm due to a number of factors including removal of biomass, organic compounds, agglutination and release of excretion products. Also, it has been claimed that the biofilm morphology in presence of grazers provides protection against predation (Huws et al., 2005). The pronounced influence of *Plectus aquatilis* on the basal layer was not described before, and should be attributed to its specific feeding pattern in sediments and on solid substrate interfaces, as shown in Fig. 8. This figure schematically depicts our hypothesis on the influence of nematodes on membrane biofilms: The nematodes graze and feed on the biofilm, acting on the entire thickness of the biofilm (from its base to its

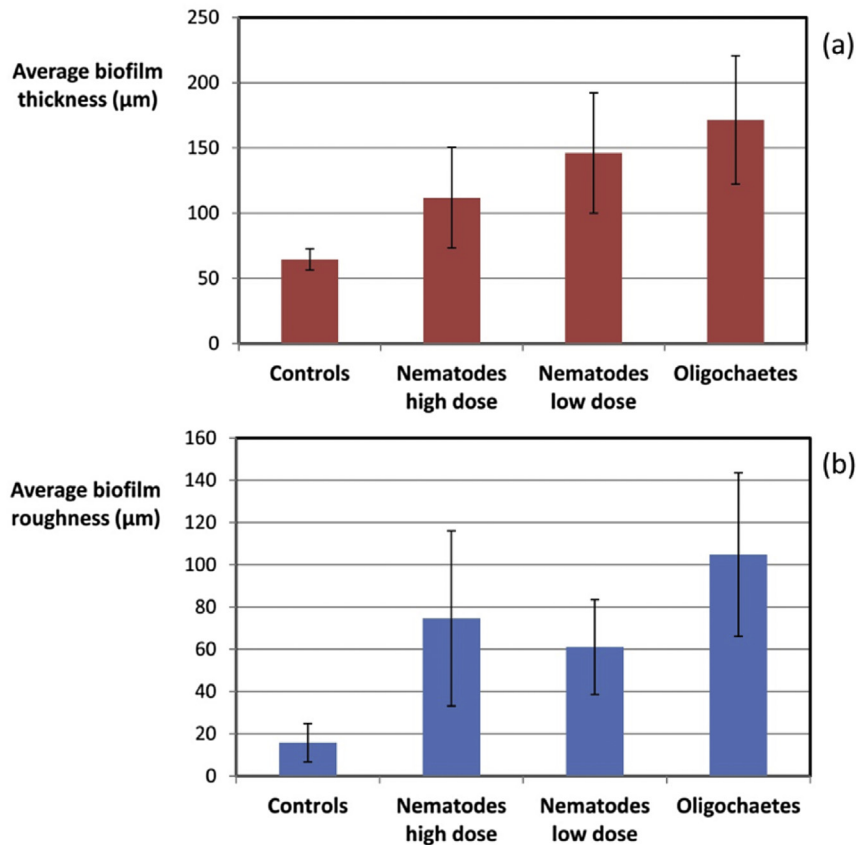


Fig. 4. Average biofilm thickness (a), and biofilm roughness (b) calculated from OCT images in the period of 40–50 days of operation. Multiple randomly chosen fields were evaluated for different modules and different points of time during the period of day 40–50. A total of 200 images were evaluated for the control system, 160 for the system with a high dose of nematodes, 160 for low dose of nematodes, and 240 for oligochaetes. Error bars show the standard deviation.

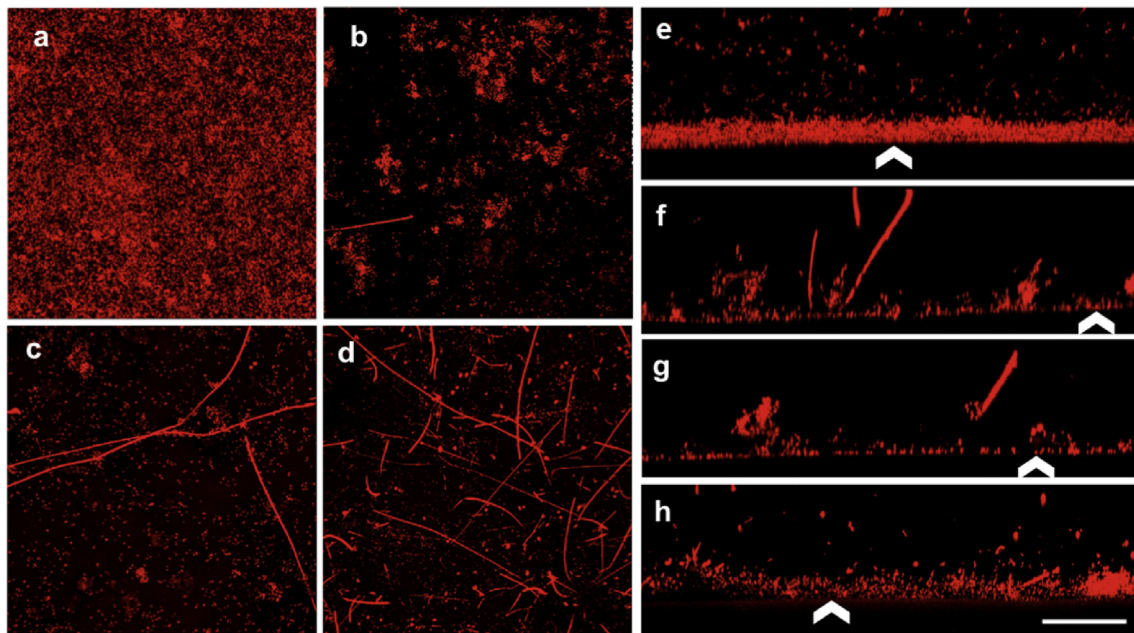


Fig. 5. Representative CLSM images showing top-views (a–d) and optical cross-sections (e–j) of the biofilm basal layer, obtained after washing-off the biofilm by cross-flow and subsequent protein staining using Sypro Orange. Images (a) and (e) represent the control system; Images (b) and (f) the system dosed with a low concentration of nematodes; Images (c) and (g) the system dosed with a high concentration of nematodes; Images (d) and (h) the system with oligochaetes. Images a–d represent the maximum projections of the X–Y–Z stack ($X = 260 \mu\text{m}$, $Y = 260 \mu\text{m}$, $Z = \text{maximum height of the basal layer}$). Images e–h represent the maximum projection of the X–Y–Z stack ($X = 260 \mu\text{m}$, $Y = \text{maximum height}$, $Z = 30 \mu\text{m}$). Arrowheads in the cross-sections indicate the location of the membrane surface. The scale bar represents $50 \mu\text{m}$. (For interpretation of the references to colour in this figure legend, the reader is referred to the web version of this article.)

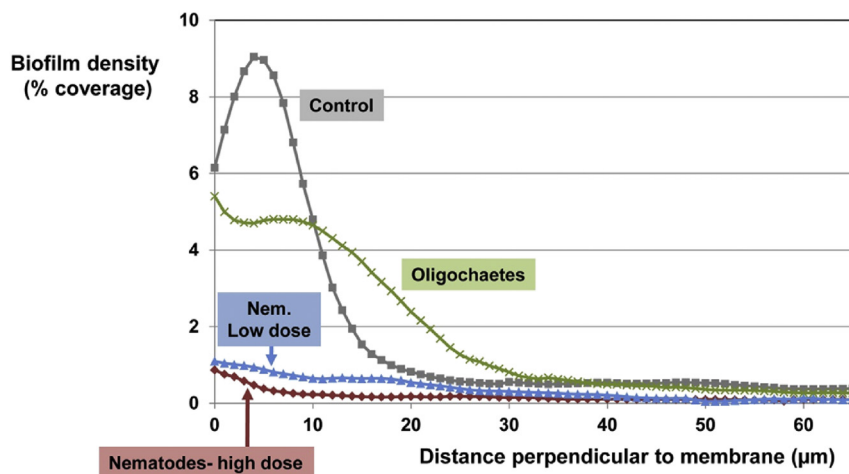


Fig. 6. Basal layer density, expressed as % area coverage of the CLSM Sypro Orange signal as a function of the distance to the membrane surface for different types of organisms as well as control systems. Data were calculated from CLSM images (z-stacks) and averaged on basis multiple randomly chosen z-stacks. (For interpretation of the references to colour in this figure legend, the reader is referred to the web version of this article.)

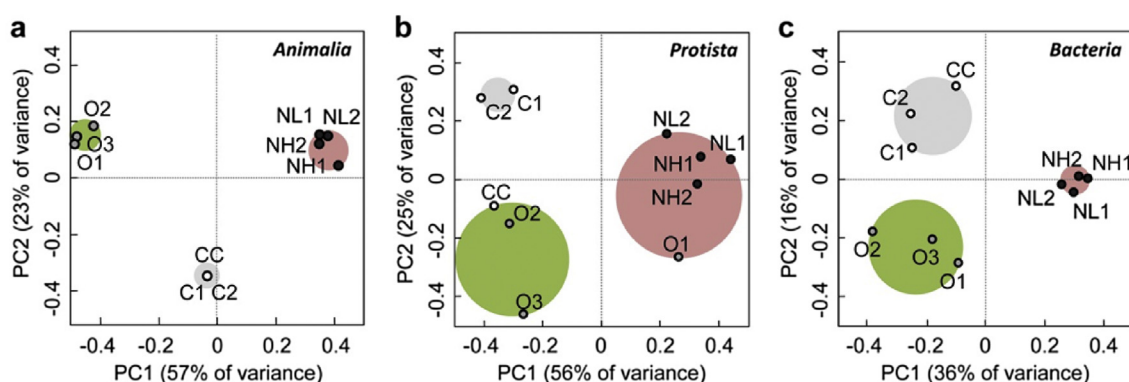


Fig. 7. Principal component analysis of communities of Animalia (a), Protista (b) and Bacteria (c). The superimposition of the colored circles is based on the hierarchical clustering analysis available in Fig. S6. C1 and C2 refer to the control systems, CC to the control with cycloheximide, NL1-2 to the low dose of nematodes, NH1-2 to the high dose of nematodes, and O1-3 to oligochaetes. (For interpretation of the references to colour in this figure legend, the reader is referred to the web version of this article.)

surface), thus affecting the structure and thickness of the basal layer as well as the structure of entire biofilm.

As discussed in Section 3.1, the high flux in presence of metazoans potentially can improve the application on decentralized scale and enable GDM application on a centralized scale. As it can be expected that the flux decreases rapidly if metazoans cease their activity, the population of metazoans should be continuously maintained during operation. Although some metazoan feeding patterns have been described the ecology of these organisms is still largely unknown. However, it can be assumed that for maintenance of the population of metazoans a continuous presence of substrates (e.g. bacteria, organic particles) is required and stress factors need to be avoided. Stress factors can include chemicals, shear forces and other chemical and physical factors (e.g. temperature, pH). These factors need to be investigated in order to enable application in practice.

Besides the UF membrane systems described here, the results may have broader implications for removal of biofilms in general, especially in cases where conventional approaches (based on chemicals, and mechanical or hydraulic shear) are not feasible. Biofilms are notorious in spiral-wound reverse osmosis (RO) membrane modules. Once they are established, they are extremely hard to remove, because the fine meshed spacers in such modules serve as a biofilm support matrix. Biological control methods with

nematodes or other metazoans could serve as an alternative to chemical methods, which have several disadvantages, including environmental incompatibility and the impact on membrane life time and integrity (Crittenden et al., 2012; Fane et al., 2006). Furthermore, biofilms can cause problems in water distribution systems and in (closed) water systems, such as cooling water systems. Also in such cases, a biological approach based on nematodes could provide a valuable alternative to chemical-based methods. As discussed in the Introduction, metazoans have been observed in MBRs, and their influence on permeability has been suggested (Jabornig and Podmirseg, 2015). While not all metazoans seem to have the same effect on flux, specific types of metazoans could be added to MBRs or conditions could be created which enable those species of metazoans to proliferate which have a positive influence on flux. Finally, biofilm removal is relevant for medical applications, because such biofilms can develop tolerance to antibiotics (Donlan, 2001). Health relevant biofilms can occur on implanted medical devices, dental plaque, in ear and lung infection (Donlan, 2001; Ferreira et al., 2009; Williams et al., 2009). Previously, it was described that some bacterial swimmers can penetrate into biofilms, enhancing the exposure to antibiotics into the depth of the biofilm, with potential application for cure of skin, nasal or intestinal infections (Houry et al., 2012). In principle, the use of nematodes can also be considered for such cases, with the additional

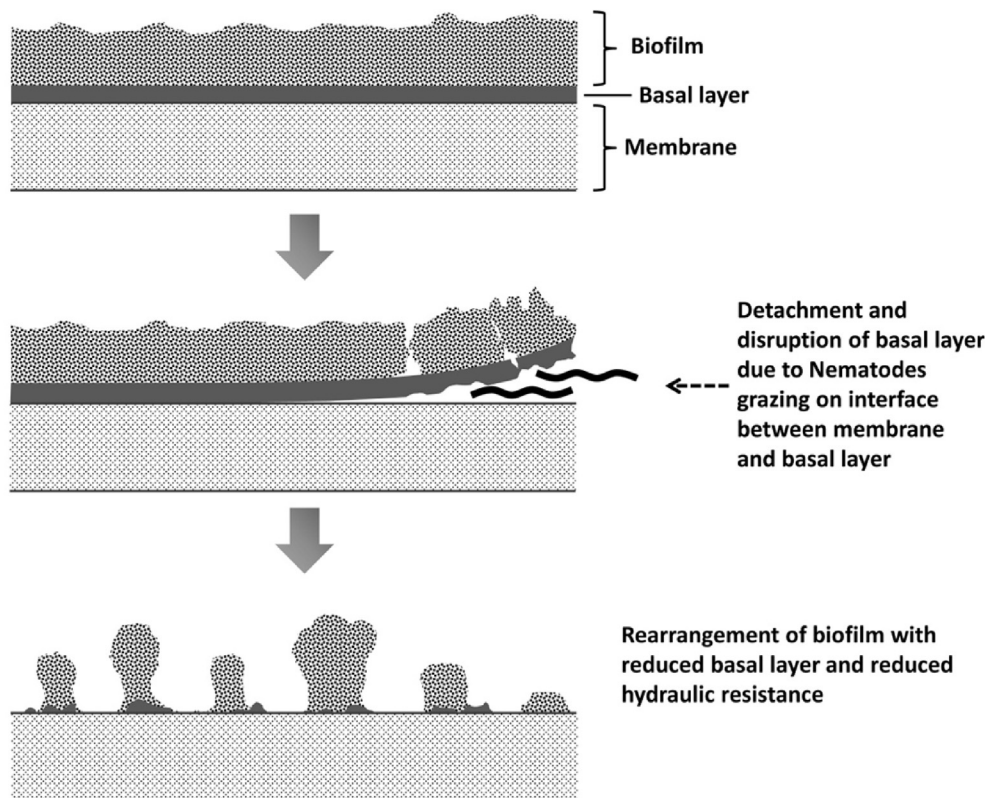


Fig. 8. Schematic representation of the impact of nematodes on the structure of the biofouling layer.

advantage of biofilm detachment and removal of the basal layer.

4. Conclusions

In this study, it was found that the presence of metazoans exerts a clear influence on the flux of biofilm-controlled membrane systems.

- In case of a high dose of nematodes the flux was in the range of 17.5–20.8 L/(m²h), while the flux was 14.0–17.7 L/(m²h) in case of a low dose of nematodes inoculated. The flux in the control systems was in the range of 5.7–8.8 L/(m²h).
- In the case of oligochaetes the flux was 9.2–12.5 L/(m²h) while the flux was 5.7–8.8 L/(m²h) in the control systems.
- The morphology of the biofouling layer was influenced by the metazoans, converting it from a flat and homogeneous layer into a heterogeneous, patchy and open porous structure in presence of nematodes or oligochaetes.
- The presence of nematodes resulted in a strong reduction of thickness and density of the basal layer, while the presence of oligochaetes resulted in a less pronounced reduction of density.
- The biological community composition of the biofilm was influenced, not only in terms of metazoans itself, but also the composition of protozoa and bacteria was significantly influenced, presumably due to the feeding and excretion patterns of the metazoans.
- The results are relevant for flux optimization of GDM systems treating potable water, grey water or wastewater, as well as MBR systems. Further research is needed to investigate these fields of application, as well as methods to sustain the metazoan population and to maintain elevated flux values during longer periods of operation.

Acknowledgements

The authors would like to thank Prof. Tony Fane for critically reviewing the manuscript, Jacqueline Traber for analytical support, and Andrea Ansell as well as Peter Desmond for linguistic corrections.

Appendix A. Supplementary data

Supplementary data related to this article can be found at <http://dx.doi.org/10.1016/j.watres.2015.09.050>.

References

- Bergtold, M., Mayr, G., Traunspurger, W., 2007. Nematodes in wastewater biofilms – appearance and density of species in three biofilter reactors. *Water Res.* 41 (1), 145–151.
- Böhme, A., Risse-Buhl, U., Küsel, K., 2009. Protists with different feeding modes change biofilm morphology. *FEMS Microbiol. Ecol.* 69 (2), 158–169.
- Borcard, D., Gillet, F., Legendre, P., 2011. *Numerical Ecology* with R. Springer.
- Brepols, C., Drensla, K., Janot, A., Trimborn, M., Engelhardt, N., 2008. Strategies for chemical cleaning in large scale membrane bioreactors. *Water Sci. Technol.* 57 (3), 457–463.
- Calderon, K., Rodelas, B., Cabirol, N., Gonzalez-Lopez, J., Noyola, A., 2011. Analysis of microbial communities developed on the fouling layers of a membrane-coupled anaerobic bioreactor applied to wastewater treatment. *Bioresour. Technol.* 102 (7), 4618–4627.
- Camacho, C., Coulouris, G., Avagyan, V., Ma, N., Papadopoulos, J., Bealer, K., Madden, T.L., 2009. BLAST+: Architecture and Applications. *BMC Bioinformatics*, p. 10.
- Crittenden, J.C., Trussell, R.R., Hand, D.W., Howe, K.J., Tchobanoglous, G., 2012. *MWH's Water Treatment: Principles and Design*, third ed. Wiley.
- Danovaro, R., Gambi, C., Dell'Anno, A., Corinaldesi, C., Fraschetti, S., Vanreusel, A., Vincx, M., Gooday, A.J., 2008. Exponential decline of deep-sea ecosystem functioning linked to benthic biodiversity loss. *Curr. Biol.* 18 (1), 1–8.
- Derlon, N., Koch, N., Eugster, B., Posch, T., Pernthaler, J., Pronk, W., Morgenroth, E., 2013. Activity of metazoans governs biofilm structure formation and enhances permeate flux during Gravity-Driven Membrane (GDM) filtration. *Water Res.* 47

- (6), 2085–2095.
- Derlon, N., Peter-Varbanets, M., Scheidegger, A., Pronk, W., Morgenroth, E., 2012. Predation influences the structure of biofilm developed on ultrafiltration membranes. *Water Res.* 46 (10), 3323–3333.
- Dodds, W.K., 2002. *Freshwater Ecology: Concepts and Environmental Applications*. Elsevier Science.
- Donlan, R.M., 2001. Biofilm formation: a clinically relevant microbiological process. *Clin. Infect. Dis.* 33 (8), 1387–1392.
- Elissen, H.J.H., Peeters, E.T.H.M., Buys, B.R., Klapwijk, A., Rulkens, W., 2008. Population dynamics of free-swimming Annelida in four Dutch wastewater treatment plants in relation to process characteristics. *Hydrobiologia* 605 (1), 131–142.
- Fane, A.G., Xi, W., Rong, W., 2006. In: Newcombe, G., Dixon, D. (Eds.), *Interface Science and Technology*. Elsevier, pp. 109–132.
- Ferreira, J.A.G., Carr, J.H., Starling, C.E.F., de Resende, M.A., Donlan, R.M., 2009. Biofilm formation and effect of caspofungin on biofilm structure of *Candida* species bloodstream isolates. *Antimicrob. Agents Chemother.* 53 (10), 4377–4384.
- Gaude, A., Munoz, I., Moens, T., 2013. Bottom-up effects on freshwater bacterivorous nematode populations: a microcosm approach. *Hydrobiologia* 707 (1), 159–172.
- Goosen, M.F.A., Sablani, S.S., Ai-Hinai, H., Ai-Obeidani, S., Al-Belushi, R., Jackson, D., 2004. Fouling of reverse osmosis and ultrafiltration membranes: a critical review. *Sep. Sci. Technol.* 39 (10), 2261–2297.
- Huws, S.A., McBain, A.J., Gilbert, P., 2005. Protozoan grazing and its impact upon population dynamics in biofilm communities. *J. Appl. Microbiol.* 98 (1), 238–244.
- Houry, A., Gohar, M., Deschamps, J., Tischenko, E., Aymerich, S., Gruss, A., Briandet, R., 2012. Bacterial swimmers that infiltrate and take over the biofilm matrix. *Proc. Natl. Acad. Sci.* 109 (32), 13088–13093.
- Isaacson, C.W. (2015) **Personal Communication**.
- Jabornig, S., Podmirseg, S.M., 2015. A novel fixed fibre biofilm membrane process for on-site greywater reclamation requiring no fouling control. *Biotechnol. Bioeng.* 112 (3), 484–493.
- Johnson, M., Zaretskaya, I., Raytselis, Y., Merezhuk, Y., McGinnis, S., Madden, T.L., 2008. NCBI BLAST: a better web interface. *Nucleic Acids Res.* 36 (Web Server issue), W5–W9.
- Judd, S., 2008. The status of membrane bioreactor technology. *Trends Biotechnol.* 26 (2), 109–116.
- Li, M., Nakhla, G., Zhu, J., 2013. Impact of worm predation on pseudo-steady-state of the circulating fluidized bed biofilm reactor. *Bioresour. Technol.* 128, 281–289.
- Mahendran, B., Lin, H., Liao, B., Liss, S.N., 2011. Surface properties of biofouled membranes from a submerged anaerobic membrane bioreactor after cleaning. *J. Environ. Eng. ASCE* 137 (6), 504–513.
- Malaeb, L., Le-Clech, P., Vrouwenvelder, J.S., Ayoub, G.M., Saikaly, P.E., 2013. Do biological-based strategies hold promise to biofouling control in MBRs? *Water Res.* 47 (15), 5447–5463.
- Menniti, A., Morgenroth, E., 2010. The influence of aeration intensity on predation and EPS production in membrane bioreactors. *Water Res.* 44 (8), 2541–2553.
- Nguyen, T., Roddick, F.A., Fan, L., 2012. Biofouling of water treatment membranes: a review of the underlying causes, monitoring techniques and control measures. *Membranes* 2 (4), 804–840.
- Pechaud, Y., Marcato-Romain, C.E., Girbal-Neuhausser, E., Queinnee, I., Bessiere, Y., Paul, E., 2012. Combining hydrodynamic and enzymatic treatments to improve multi-species thick biofilm removal. *Chem. Eng. Sci.* 80, 109–118.
- Peter-Varbanets, M., Gujer, W., Pronk, W., 2012. Intermittent operation of ultra-low pressure ultrafiltration for decentralized drinking water treatment. *Water Res.* 46 (10), 3272–3282.
- Peter-Varbanets, M., Hammes, F., Vital, M., Pronk, W., 2010. Stabilization of flux during dead-end ultra-low pressure ultrafiltration. *Water Res.* 44 (12), 3607–3616.
- Peter-Varbanets, M., Johnston, R., Meierhofer, R., Kage, F., Pronk, W., 2011. In: Shaw, R. (Ed.), *Gravity-driven Membrane Disinfection for Household Drinking Water Treatment*. WEDC, Loughborough, UK, ISBN 978 1 84380 142 9.
- Quast, C., Pruesse, E., Yilmaz, P., Gerken, J., Schweer, T., Yarza, P., Peplies, J., Glöckner, F.O., 2013. The SILVA ribosomal RNA gene database project: improved data processing and web-based tools. *Nucleic Acids Res.* 41 (D1), D590–D596.
- Riemann, F., Helmke, E., 2002. Symbiotic relations of sediment-agglutinating nematodes and bacteria in detrital habitats: the enzyme-sharing concept. *Mar. Ecol. Pubbl. Della Stn. Zool. Napoli* 1 23 (2), 93–113.
- Seigneur, C., Calvelo, J., Adler, N., Holliger, C., 2004. Control of Biomass Growth by Nematode-grazing Bacteria in a Biofilter Treating Chlorobenzenes. A. A. Balkema Publishers, Leiden.
- Song, B.Y., Chen, X.F., 2009. Effect of *Aeolosoma hemprichi* on excess activated sludge reduction. *J. Hazard. Mater.* 162 (1), 300–304.
- Sun, Y., Wolcott, R., Dowd, S., 2011. In: Kwon, Y.M., Ricke, S.C. (Eds.), *High-throughput Next Generation Sequencing*. Humana Press, pp. 129–141.
- Tamis, J., van Schoutvenburg, G., Kleerebezem, R., van Loosdrecht, M.C.M., 2011. A full scale worm reactor for efficient sludge reduction by predation in a wastewater treatment plant. *Water Res.* 45 (18), 5916–5924.
- Wang, Q.Y., Wang, Z.W., Wu, Z.C., Han, X.M., 2011. Sludge reduction and process performance in a submerged membrane bioreactor with aquatic worms. *Chem. Eng. J.* 172 (2–3), 929–935.
- Wei, Y.S., Wang, Y.W., Guo, X.S., Liu, J.X., 2009. Sludge reduction potential of the activated sludge process by integrating an oligochaete reactor. *J. Hazard. Mater.* 163 (1), 87–91.
- Weissbrodt, D.G., Shani, N., Holliger, C., 2014. Linking bacterial population dynamics and nutrient removal in the granular sludge biofilm ecosystem engineered for wastewater treatment. *FEMS Microbiol. Ecol.* 88 (3), 579–595.
- Williams, M.M., Yakus, M.A., Arduino, M.J., Cooksey, R.C., Crane, C.B., Banerjee, S.N., Hilborn, E.D., Donlan, R.M., 2009. Structural analysis of biofilm formation by rapidly and slowly growing nontuberculous mycobacteria. *Appl. Environ. Microbiol.* 75 (7), 2091–2098.
- Wu, C.Y., Ushiwaka, S., Horii, H., Yamagiwa, K., 2008. Membrane-attached biofilm as a mean to facilitate nitrification in activated sludge process and its effect on the microfaunal population. *Biochem. Eng. J.* 40 (3), 430–436.
- Zhang, J., Padmasiri, S.I., Fitch, M., Norddahl, B., Raskin, L., Morgenroth, E., 2007. Influence of cleaning frequency and membrane history on fouling in an anaerobic membrane bioreactor. *Desalination* 207 (1–3), 153–166.